AD A185 433 PROPELLER DESIGN OF US NAVY'S SWATH (SMALL WATERPLANE AREA TWIN HULL) T-AGOS 19(U) DAVID W TAYLOR NAVAL SHIP RESEARCH AND DEVELOPMENT CENTER BEEHESDA MD 1/1

UNCLASSIFIED K KIM ET AL. AUG 87 DTNSRDC-87/034 F/G 13/10 NL

END
11 87
DTIC

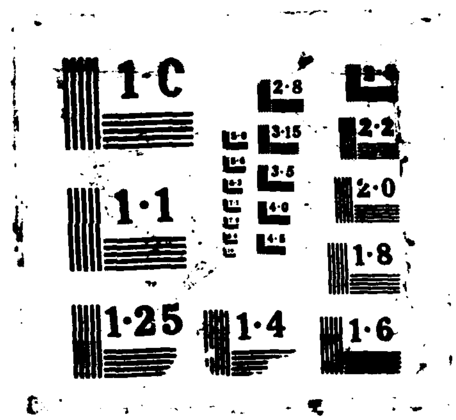

2·8
3·15
3·5
4·0
4·5
2·2
2·0
1·1
1·8
1·25
1·4
1·6

David W. Taylor Naval Ship Research and Development Center
Bethesda, MD 20084-5000

DTNSRDC-87/034 August 1987

Ship Hydromechanics Department
Research and Development Report

Propeller Design of U.S. Navy's SWATH T-AGOS 19

by

Ki-Han Kim

Arthur M. Reed

Presented at the Third International Symposium on
Practical Design of Ships and Mobile-Units (PRADS '87)
Trondheim, Norway, 20-25 June 1987

Approved for public release; distribution is unlimited.

DTNSRDC-87/034 Propeller Design of U.S. Navy's SWATH T-AGOS 19

UNCLASSIFIED
SECURITY CLASSIFICATION OF THIS PAGE

AD-D013 433

REPORT DOCUMENTATION PAGE

1a. REPORT SECURITY CLASSIFICATION: UNCLASSIFIED	1b. RESTRICTIVE MARKINGS
2a. SECURITY CLASSIFICATION AUTHORITY	3. DISTRIBUTION/AVAILABILITY OF REPORT: Approved for public release; distribution is unlimited.
2b. DECLASSIFICATION/DOWNGRADING SCHEDULE	
4. PERFORMING ORGANIZATION REPORT NUMBER(S): DTNSRDC-87/034	5. MONITORING ORGANIZATION REPORT NUMBER(S)
6a. NAME OF PERFORMING ORGANIZATION: David W. Taylor Naval Ship Research & Development Center; 6b. OFFICE SYMBOL (If applicable): Code 1544	7a. NAME OF MONITORING ORGANIZATION
6c. ADDRESS (City, State, and ZIP Code): Bethesda, MD 20084-5000	7b. ADDRESS (City, State, and ZIP Code)
8a. NAME OF FUNDING/SPONSORING ORGANIZATION: Naval Sea Systems Command; 8b. OFFICE SYMBOL (If applicable): SEA 5046	9. PROCUREMENT INSTRUMENT IDENTIFICATION NUMBER
8c. ADDRESS (City, State, and ZIP Code): Crystal City, Washington D.C. 20362	10. SOURCE OF FUNDING NUMBERS: PROGRAM ELEMENT NO 64567N; PROJECT NO WR10511; TASK NO S1803528; WORK UNIT ACCESSION NO DN506007

11 TITLE (Include Security Classification)
PROPELLER DESIGN OF U.S. NAVY'S SWATH, T-AGOS 19

12 PERSONAL AUTHOR(S)
Kim, Ki-Han and Reed, Arthur M.

13a TYPE OF REPORT	13b TIME COVERED	14 DATE OF REPORT (Year, Month, Day)	15 PAGE COUNT
Final	FROM 4/86 TO 4/87	1987 August	24

16 SUPPLEMENTARY NOTATION
Presented at the Third International Symposium on Practical Design of Ships and Mobile Units (PRADS '87), Trondheim, Norway, 20-25 June 1987

17 COSATI CODES			18 SUBJECT TERMS (Continue on reverse if necessary and identify by block number)
FIELD	GROUP	SUB-GROUP	Propeller Design, SWATH, Lifting-Surface, Lifting-Line, Blade Surface Cavitation

19 ABSTRACT (Continue on reverse if necessary and identify by block number)

This paper presents the design process and model evaluation of a propeller for the U.S. Navy's research vessel, T-AGOS 19, with a SWATH (Small Waterplane Area Twin Hull) Configuration. The design procedure is discussed in detail including considerations of cavitation and propeller-excited vibratory forces. The design objective was to minimize the blade cavitation at various operating conditions. Model experimental results including powering and cavitation characteristics are presented which confirm the validity of the design process.

20 DISTRIBUTION/AVAILABILITY OF ABSTRACT: ☒ UNCLASSIFIED/UNLIMITED ☐ SAME AS RPT ☐ DTIC USERS	21 ABSTRACT SECURITY CLASSIFICATION: UNCLASSIFIED
22a NAME OF RESPONSIBLE INDIVIDUAL: Ki-Han Kim and Arthur M. Reed	22b TELEPHONE (Include Area Code): (202) 227-4308; 22c OFFICE SYMBOL: Code 1544

DD FORM 1473, 84 MAR — 83 APR edition may be used until exhausted. All other editions are obsolete.

SECURITY CLASSIFICATION OF THIS PAGE
UNCLASSIFIED

CONTENTS

A-1

FIGURES

TABLES

ADMINISTRATIVE INFORMATION

This project was carried out for the Naval Sea Systems Command under Work Request N00024-86-WR-10511. The work was performed at the David W. Taylor Naval Ship Research and Development Center under Work Unit number 1235-680.

PROPELLER DESIGN OF U.S. NAVY'S SWATH, T-AGOS 19

Ki-Han Kim and
Arthur M. Reed

David W. Taylor
Naval Ship Research
and Development Center

U.S.A.

1. ABSTRACT

This paper presents the design process and model evaluation of a propeller for the U.S. Navy's research vessel, T-AGOS 19, with a SWATH (Small Waterplane Area Twin Hull) configuration. The design procedure is discussed in detail including considerations of cavitation and propeller-excited vibratory forces. The design objective was to minimize the blade cavitation at various operating conditions. Model experimental results including powering and cavitation characteristics are presented which confirm the validity of the design process.

2. INTRODUCTION

At the request of the U.S. Naval Sea Systems Command (NAVSEA), the David W. Taylor Naval Ship Research Center (DTNSRDC) carried out a propeller design for a research vessel, T-AGOS 19, having a Small-Waterplane-Area-Twin-Hull (SWATH) configuration as shown in Figure 1. Each lower hull has inboard canard and stabiliser, fore and aft, respectively, acting as control surfaces. The droop angles for canards and stabilisers are 20 degrees and 18 degrees, respectively, relative to the baseline. The propellers are protected by ring-shaped propeller guards, each with four supporting struts (see Figure 2). The details of the ship design are presented in Reference 1. The principal characteristics of the ship are listed in Table 1. The main objective was to design a propeller with minimum cavitation resulting from the propeller operating in the spatially non-uniform inflow velocity field in the ship's wake at different operating conditions.

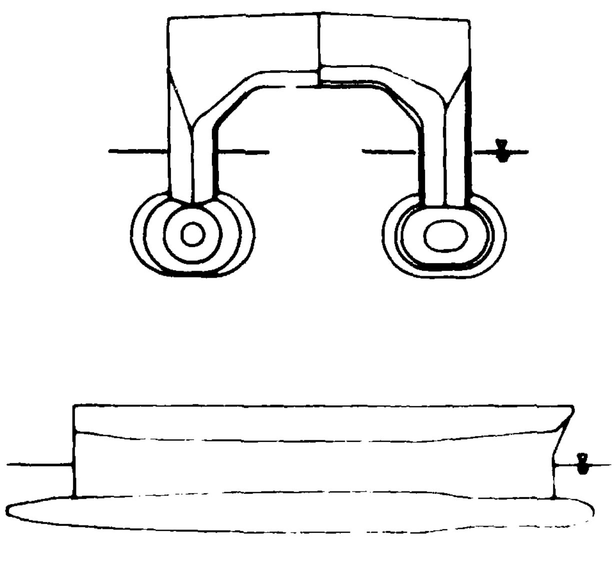

Fig. 1 Sketch of SWATH T-AGOS 19 Configuration

This paper presents the design procedure and rationale which led to the final five-bladed propeller with a 10-foot (3.05 m) diameter, and the results of powering and cavitation tests with the design propeller. The following sections describe the specified design conditions, the pertinent information required as input to the design problem such as wake survey and propulsion characteristics, the design procedure, performance prediction and powering and cavitation test results.

Table 1. Principal Characteristics of SWATH T-AGOS 19

Length Overall (LOA)	71.32 m (234 ft)
Length at Waterline (LWL)	57.91 m (190 ft)
Beam on Design Waterline	24.38 m (80 ft)
Beam (Maximum)	28.35 m (93 ft)
Draft	7.54 m (24.75 ft)
Displacement	3366 Metric Tons
Wetted Surface Area	2814 m^2

3. PROPELLER DESIGN REQUIREMENTS

The design requirements for the T-AGOS 19 propeller were provided by NAVSEA: propeller geometry should be as simple as possible, minimize the cavitation on the propeller operating at full power of 800 SHP (597 kW) per shaft, sustained speed a minimum of 9 knots at 80 percent of the full power, propeller rotational speed of 185 rpm at full power in calm water, maximum propeller diameter of 11 feet (3.35 m) with 1.5 feet (0.46 m) clearance between the propeller tip and the propeller guard. The depth of immersion of the shaft centerline in calm water is 16 feet 9 inches (5.11 m) with even keel condition.

The full-scale propeller material will be Nickel-Aluminum-Bronze alloy, American Bureau of Shipping (ABS) Grade 4. The propeller strength requirements will follow ABS 1985 Class C Ice Strengthening rules.

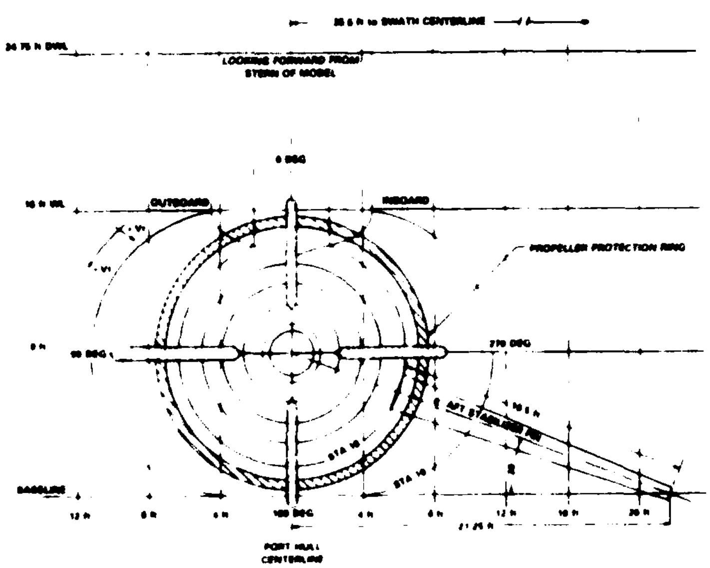

Fig. 2 Schematic Drawing of Stabilizing Fin and Propeller Guard Fins

4. WAKE SURVEY AND PROPULSION EXPERIMENTS USING STOCK PROPELLERS

The wake survey, resistance and self-propulsion tests were conducted in the DTNSRDC towing tank using Model 5445 representing the SWATH T-AGOS 19 with scale ratio of 12.5. The nominal wake was measured at model conditions corresponding to design draft, zero trim and model speed equivalent to 10 knots (5.14 m/s) full-scale. The model was fully appended with canards, stabilizers, and ring-shaped propeller guards with supporting fins. For the wake survey, canards and stabilizers were fixed at zero degree angle of attack.

The measured values of the circumferential variation in the axial, tangential and radial velocity components at four nondimensional radii are shown in Figure 3. From these data, similar results are obtained for other radii by interpolation. The sign convention of the velocity components are shown in Figure 2.

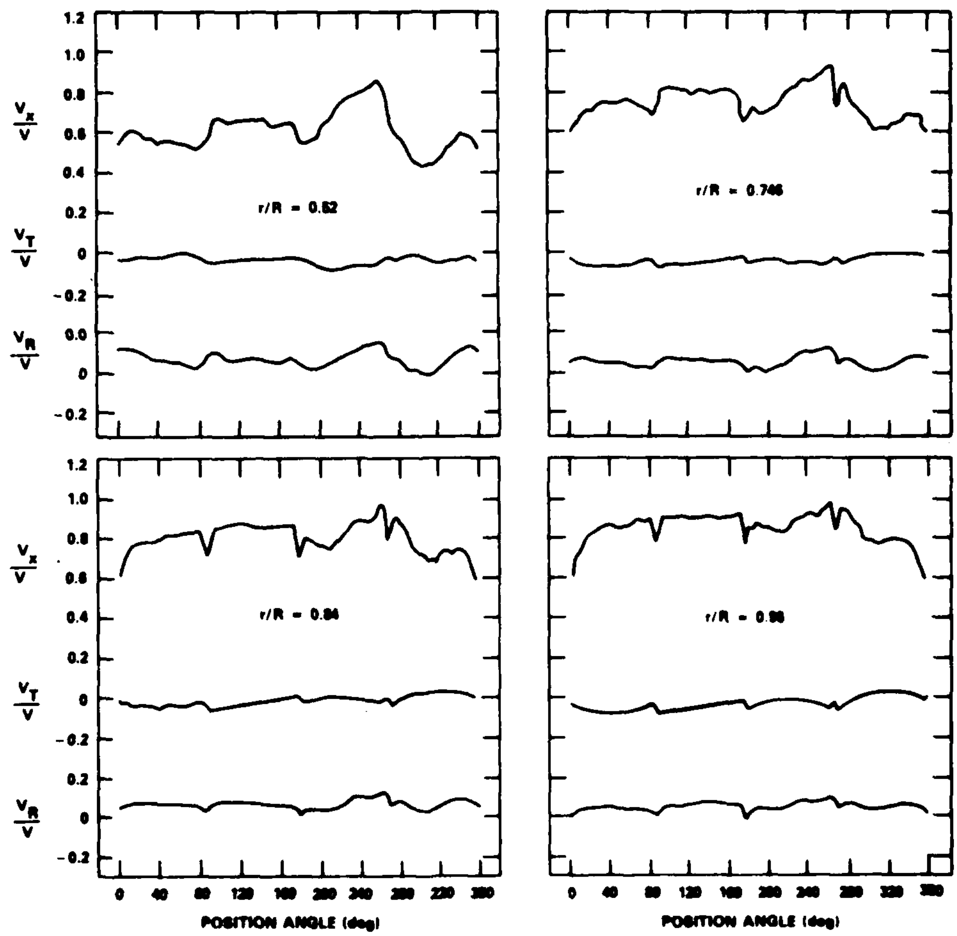

Fig. 3 Circumferential Variation in the Axial, Tangential and Radial Velocity Components

Table 2. Powering Predictions Based on Model Propulsion Test Using Stock Propellers

SHIP SPEED (KNOTS)	EHP(P_E)	DHP(P_D)	η_R	RPM	1-t	1-w_T
3.0	27.1	45.	.975	39.9	.83	.810
4.0	60.5	100.	.975	52.3	.83	.810
5.0	116.6	190.	.980	65.2	.83	.815
6.0	202.5	330.	.980	78.4	.83	.815
7.0	320.0	520.	.980	91.2	.83	.815
8.0	480.0	785.	.980	104.6	.83	.815
9.0	700.0	1140.	.985	118.4	.83	.815
10.0	955.0	1550.	.985	131.4	.83	.815
11.0	1230.0	2000.	.985	143.8	.83	.825
12.0	1580.0	2560.	.990	157.1	.83	.835

The resistance and self-propulsion experiments were performed on Model 5445 using the stock propellers. The appendage suit was the same as for the wake survey except that the angles of the control surfaces were adjusted to the position which required minimum delivered power at full-scale speed of 10 knots. The angle of attack on the forward canards was 4 degrees trailing-edge down, and for the aft stabilizers it was 6 degrees trailing-edge up. The powering predictions made by the standard DTNSRDC prediction method [2] are presented in Table 2.

5. PROPELLER DESIGN

5.1 Design Condition and Procedure

The propeller was designed to absorb 800 horsepower per shaft at 185 rpm based on the results of wake survey, and resistance and propulsion tests with stock propellers.

The propeller was designed in five phases;

(a) Preliminary Design: Estimates are made for number of blades, diameter, blade area ratio and blade outline at design condition such that the propeller is compatible with the ship and the propulsion machinery from the standpoint of efficiency and vibration.

(b) Lifting-Line Design: The radial load and the corresponding hydrodynamic pitch distributions are computed using Lerbs [3] induction factor method.

(c) Propeller Global Geometry: The initial blade chord length and the thickness distribution are refined by considering various hydrodynamic as well as structural aspects such as cavitation, erosion and thrust breakdown, and blade strength. Lifting-line calculations are repeated for different geometries as the geometry is refined.

(d) Lifting-Surface Design: The final pitch and camber distributions are determined by lifting-surface calculations.

(e) Design Check: In this phase the unsteady forces and moments are calculated and compared with the design requirements. If the predicted values do not meet the design requirement, the skew distribution is modified. Since the skew distribution will affect the resulting pitch and camber distribution, the lifting-surface calculations must be repeated for a new skew distribution. The design propeller is reviewed to check the off-design performance and to summarize the final design predictions in terms of required speed margins and other specified constraints.

These phases are specified as a guide to the major steps in the design procedure. However, most of these steps are closely interrelated, and iterations between the steps are necessary.

5.2 Estimation of Full-Scale Wake

One of the essential pieces of information for propeller design is the ship's wake in which the propeller will be operating. Two aspects must be considered for ship's wake; the effect of Reynolds number for full-scale ship and the effect of propeller action.

The effect of different Reynolds numbers, or scale effects, are important for ships such as commercial ships, SWATHs and naval auxiliaries where the propeller operates in the boundary layer of the ship's hull. There is no reliable universal method that is applicable to surface ship wake scaling. Simple methods including the one proposed by Sasajima and Tanaka [4] are available, but none of them fully represents the complicated flow behind the ship.

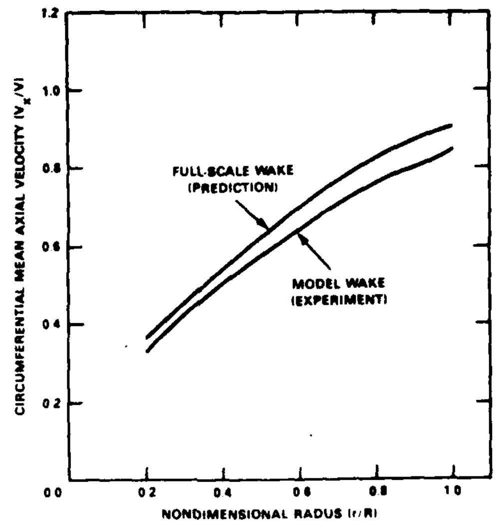

Fig. 4. Comparison of Measured Model Nominal Wake and Predicted Full-Scale Nominal Wake.

In the present design, the full-scale nominal wake was approximated by adding to the measured SWATH model nominal wake the difference between the computed model- and full-scale wake for the equivalent axisymmetric unappended hull. The nominal wake of a body of revolution was calculated based on the potential flow/boundary layer interaction theory developed by Huang, et al [5]. The submerged lower hull of T-AGOS 19 excluding the strut was approximated by an unappended body of revolution having the same length and displacement as the T-AGOS 19 hull excluding the strut. Figure 4 shows the comparison of the circumferential average of the measured model nominal wake and computed full-scale nominal wake.

When a propeller operates behind a ship, the inflow to the propeller is changed due to the action of the propeller. The propeller accelerates the flow over the stern, thus resulting in a decrease in the pressure on the hull and changes the boundary layer characteristics. This inflow to the propeller when the propeller is operating is called effective wake.

Although one can use Huang's method to calculate the effective wake, an average correction method was used in the present design. This method has proven reasonably successful in the past at DTNSRDC for obtaining the desired ship speed and shaft rpm at design power. This method uses the ratio of the effective wake, $1-w_T$, based on the thrust identity from the propulsion experiment using a stock propeller, and the volumetric mean wake, $1-w_v$, from the wake survey, i.e.:

$$(V_x/V)_{Corrected} = (V_x/V)_{Nominal} \times \frac{(1 - w_T)}{(1 - w_v)} \qquad (1)$$

where V_x/V is the nondimensional circumferential mean, axial velocity component from the wake survey.

To account for scale effects, the effective wake of the full-scale ship was empirically estimated by increasing the model effective wake by 6 percent. The radial distribution of the full-scale effective wake was also estimated by using Equation (1). For final propeller design, the corrected full-scale wake distribution was used.

5.3 Diameter Optimization

The propeller diameter was determined by considering the propulsive efficiency at full power and low speeds with different propeller loadings and the sustained speed requirement. The propulsive efficiency was calculated by a lifting-line procedure for these conditions. For each operating condition, the propeller diameter was varied from 8 to 11 feet. In these calculations the radial load distribution was assumed to be Lerbs optimum for all conditions.

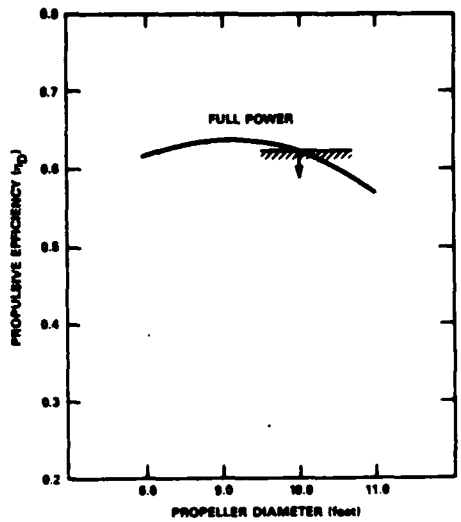

Fig. 5. Propulsive Efficiency at Different Operating Conditions for Different Diameter.

As shown in Figure 5, the optimum diameter for the full power condition is about 9 feet. Although not shown in this figure, the optimum diameter increases with increasing loading at low speed. Therefore, considering the low speed conditions the diameter was taken as maximum allowable which satisfies the sustained speed requirement. With a 5 percent speed margin added to the minimum required sustained speed of 9.0 knots, the effective power is 800 horsepower and the required propulsive efficiency is 0.625. From Figure 5, the maximum diameter which satisfies the propulsive efficiency of 0.625 at the sustained speed of 9.45 knots is 10 feet. In the following analysis, the propeller diameter was set to 10 feet.

5.4 Circulation Distribution

Three circulation distributions were investigated as shown in Figure 6. The corresponding hydrodynamic pitch angle, tan are also shown in Figure 6. The Lerbs optimum circulation distribution, designated G_0, and the mathematically unloaded root and tip circulations were investigated to serve as a guide to select the degree of tip unloading. Lerbs optimum is an estimate of the circulation distribution which will produce the highest efficiency for a wake-adapted propeller.

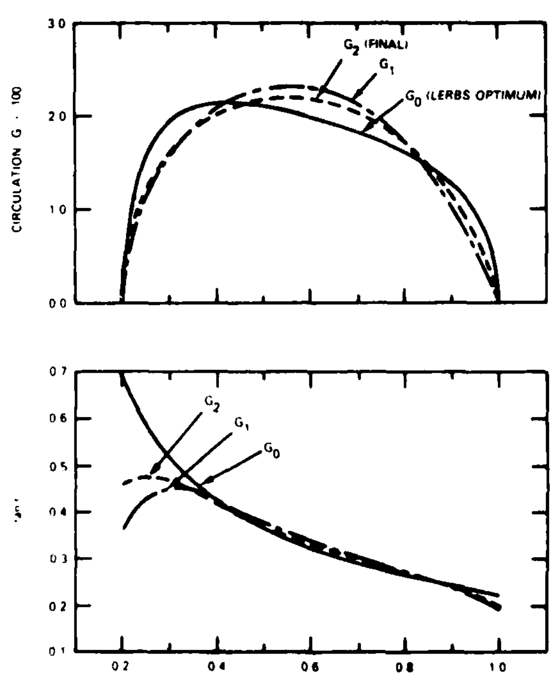

Fig. 6. Circulation and $\tan\beta_i$ Distributions.

Table 3 shows the speed predicted by the lifting-line program at full power for the three circulation distributions for the same diameter of 10 feet and the expanded area ratio (EAR) of 0.4. Load distribution G_2 was selected as final which represents a calculated sacrifice in ship speed at full power of 0.02 knots as compared to the Lerbs optimum propeller.

5.5 Thickness and Chord Length Distribution

The thickness and chordlength distributions should be carefully selected to provide adequate blade strength and simultaneously minimize the tendency towards cavitation erosion. In addition, the propeller efficiency must not be materially sacrificed.

Table 3. Effect of Radial Circulation Distribution on Propeller Performance

TYPE OF CIRCULATION	SHIP SPEED (KNOTS) RPM = 185	PROPULSIVE EFFICIENCY
Go (OPTIMUM)	10.17	0.624
G1	10.13	0.615
G2 (FINAL)	10.15	0.619

In order to select a blade shape for best cavitation characteristics, use was made of theoretically predicted cavitation inception data for two-dimensional sections [6]. For a given blade shape, i.e., c/D and consequently t/c, the cavitation characteristics were evaluated by calculating the angle of attack variation with cavitation number, and comparing it with the minimum pressure envelopes, which are commonly called "cavitation buckets".

The minimum thickness was determined first according to the 1985 ABS Class C, Ice Strengthening Rule [7]. The initial shape of the chord length distribution was taken from the existing DTNSRDC Propeller 4381 [8]. The radial distributions of c/D and t/c have been varied until the prediction ensured no leading edge and back bubble cavitations at the design condition. The final thickness and chord length distributions thus obtained are shown in Figures 7 and 8, respectively. The resulting expanded area ratio was 0.484.

5.6 Lifting-Line Design

Since we have sufficient information on geometry, ship wake and powering characteristics, a more elaborate design can be made using lifting-line model to predict the ship speed, effective power, blade lift coefficients at design condition, and other information necessary for lifting-surface design. In the lifting-line calculations, viscous effects are included by specifying the sectional drag coefficient, C_D. In the present design, full-scale section

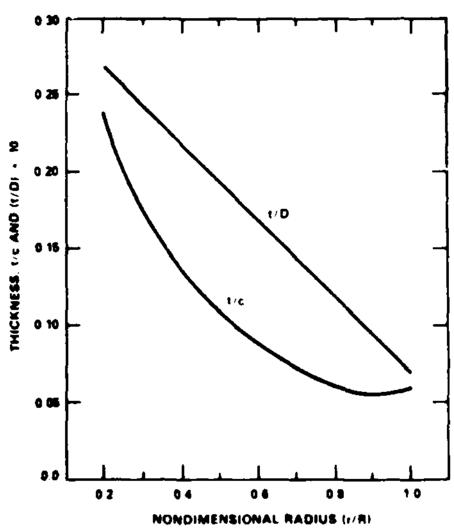

Fig. 7. Radial Distribution of Thickness.

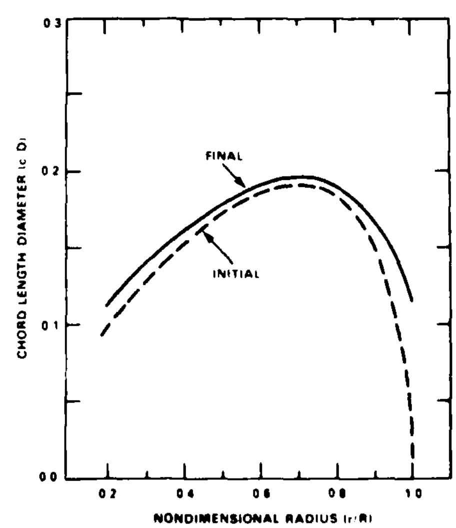

Fig. 8. Radial Distribution of Chord Length.

drag coefficients were used based on the experimental and empirical data in Reference 9. The C_D value at 0.7 radius was 0.0066. The predicted ship speed at the full power design condition is 10.24 knots and the thrust coefficient, K_T, is 0.103.

5.7 Lifting-Surface Design

The final pitch and camber distributions corresponding to the selected radial load distribution and other geometry from lifting-line computations were determined from lifting-surface computations using the computer code, PBD-10, developed by Greeley and Kerwin [10]. The section thickness shape was selected as NACA 66 with NSRDC modified nose and tail [6] and camber as NACA a=0.8 meanline.

Figures 9 and 10 show the final pitch and camber distributions determined from lifting-surface code together with the values computed from lifting-line code. Table 4 presents a summary of the design propeller geometry. Figure 11 shows the blade outline of the design propeller.

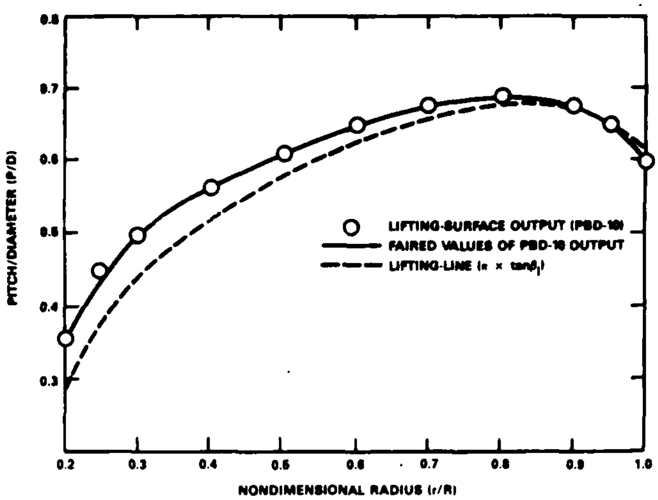

Fig. 9. Pitch Distribution (P/D) Predicted by Lifting-Surface Code, PBD-10.

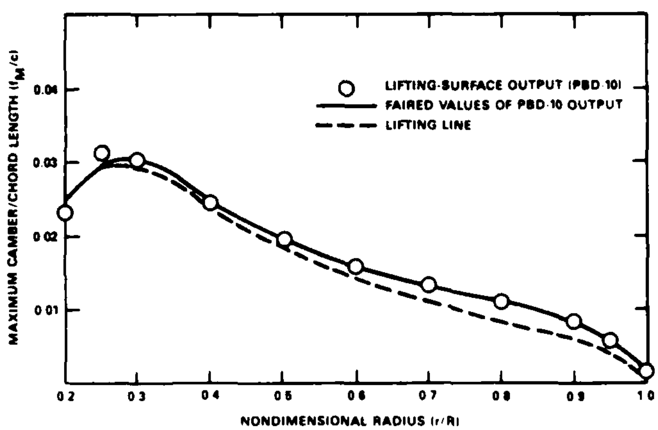

Fig. 10. Final Camber Distribution (f_M/c) Predicted by Lifting-Surface Code, PBD-10.

6. PERFORMANCE PREDICTION

6.1 Prediction of Delivered Power and RPM

In order to predict the delivered power and propeller rpm, open-water performance is necessary. The open-water performance of the design propeller was predicted by using lifting-surface computer code, PSF-2, developed by Greeley and Kerwin [10].

Once the design propeller open-water performance and the stock propeller powering characteristics are known, the propeller rotational speed and the delivered power can be estimated assuming that the propeller/hull interaction coefficients, (1-t) and $(1-w_T)$, and the relative rotative efficiency, η_R, are same for both the stock and the design propellers.

Then, the shaft power can be obtained from the effective power and the propulsive efficiency. For a given ship speed, the advance coefficient was obtained from the intersection of K_T/J^2 curve and the propeller open-water curve; K_T versus J. From this advance coefficient, the propeller rotational speed was computed.

At full power, the predicted ship speed was 10.45 knots and the propeller rpm was 186.2. The discrepancy may be caused by inaccuracy in the predicted open-water performance.

6.2 Unsteady Bearing Forces and Moments

The unsteady bearing forces and moments are calculated by using a lifting-surface code, PUF-2, developed by Kerwin and Lee [11]. The predicted fundamental blade-frequency (5th harmonic) thrust and torque values were 5.74% and 4.33% of the design thrust (K_T=0.1031) and torque (K_Q=0.012) values, respectively. Since the basic design criterion was to produce a simplest possible blade geometry, no attempt has been made to incorporate skew in order to reduce the calculated unsteady forces and moments.

Table 4. Geometric Characteristics of Design Propeller of SWATH T-AGOS 19

Diameter	3.05 m (10 ft)
Number of Blades	5
Rotational Direction	Outward
Expanded Area Ratio	0.4276
P/D at 0.7R	0.6471
Section Meanline	NACA a=0.8
Section Thickness	NACA 66 (Mod.)
Design Advance Coeff.	J_A = 0.484
Design Thrust Coeff.	K_T = 0.103
Thrust Loading Coeff.	C_T = 0.835

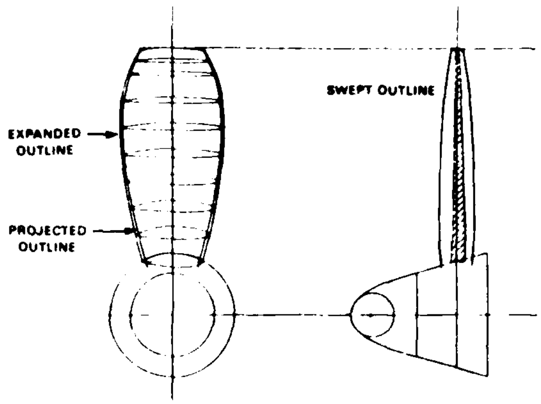

Fig. 11. Blade Outline of Design Propeller.

7. EXPERIMENTAL RESULTS AND ADJUSTMENT OF BLADE PITCH

7.1 Open-Water and Powering Experiments

Three aluminum model propellers; one with a diameter of 12 inches for cavitation tests, and two with a diameter of 9.6 inches for powering tests, were manufactured by Maritime Research & Consulting (SSPA) in Sweden. The open-water and powering experiments were carried out at DTNSRDC. The predictions of full-scale powering performance based on the model tests with the design propellers are summarized in Table 5.

The predicted full-scale rpm was about 5 rpm lower than the design rpm of 185. The major cause of this low rpm is presumably due to the large difference in Taylor wake fraction ($1-w_T$) between stock propeller test (0.864 for full-scale wake), which was used for the design, and the wake fraction obtaianed from the test with the design propeller (0.755 for full-scale wake). The effective wake, $1-w_T$, from stock propeller test is about 15% higher than the value from design propeller test. As a result the design propeller is overpitched and turns at a slower speed than the design rpm. Since 5 rpm was out of acceptable range, it was decided to modify the propeller geometry.

7.2 Adjustment of Blade Pitch

A simple way of correcting the low rpm is to reduce the pitch by rotating the blades about the blade reference line so that the new rpm will match the design rpm. In order to determine a new pitch distribution which will produce 185 rpm at full power, three rotational angles; 1.0, 0.5 and 0.6 degrees in

order, were tested. The new pitch was obtained by reducing pitch by the same pitch angle at all radii. For each new pitch, the open-water performance was calculated by PSF-2.

The rpm's for the repitched propellers were calculated based on the predicted open-water performance of the repitched propellers and the powering test results for the original propeller, with the assumption that the propeller/hull interaction coefficients were same for both the original and the repitched propellers. Table 6 shows the predicted rpm of the repitched propellers. For the same prediction conditions, the difference in predicted rpm between the original propeller and the propeller repitched by 0.6 degrees is 5.0.

Based on this parametric study, the pitch of the original propeller was reduced at SSPA by rotating the blades about the blade reference line by 0.6 degrees. Figure 12 and 13 show the comparison of the pitch distributions and the experimental open-water performance of the original and the repitched propellers, respectively.

A new power and rpm prediction was made for the repitched propeller utilizing the open-water test results, and assuming the propeller-hull interaction coefficients and the propulsive coefficients were the same as for the original propeller.

Table 5. Predicted Full-Scale Speed and RPM at Full Power Based on Model Tests Using Design Propeller

Full Power 1600 HP	With Still Air Drag	Without Still Air Drag
V (Knots)	10.49	10.56
RPM	180.0	179.9
$1-w_T$	0.755	0.755
1-t	0.820	0.820

Table 6. Predicted RPM for Original Design and Repitched Propellers at Full Power

PROPELLER	RPM
Original Propeller	181.3
Repitched Propeller (1.0 degree)	190.5
Repitched Propeller (0.5 degree)	185.2
Repitched Propeller (0.6 degree)	186.3

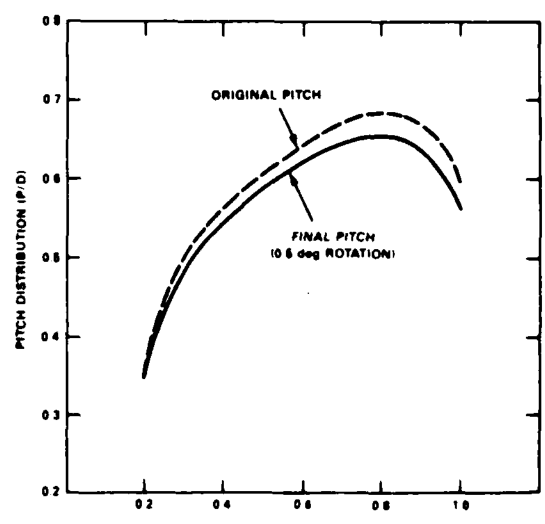

Fig. 12. Comparison of the Original and Final Pitch Distribution

Figure 14 shows the comparison of the predicted full-scale power and rpm for the original and the repitched propellers. At full power, the full-scale rpm and the ship speed for the repitched propeller were predicted to be 184.8 and 10.4 knots, respectively. Based on this prediction, NAVSEA decided to accept the repitched propeller as the final propeller for SWATH T-AGOS 19. No propulsion tests were carried out using the repitched propeller.

7.3 Cavitation Tests

Wake survey and cavitation tests were carried out in the SSPA's large cavitation tunnel (cross section 2.6m x 1.15m) with a complete starboard demihull mounted in the test section on the design waterline [12]. The demihull model was equipped with the canard, stabilizer, and the propeller protection ring with its four support guards.

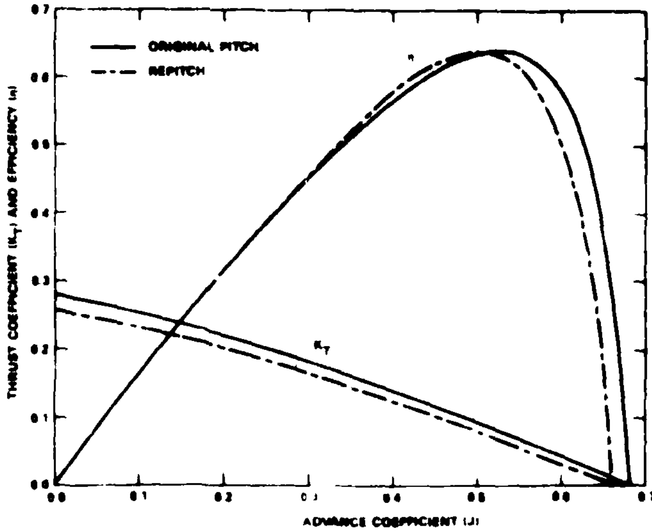

Fig. 13 Comparison of Experimental Open Water Performances between Original and Repitched Propellers

Wake measurements were performed using 5-hole pitot tubes with the optimum angle of attack for the control surfaces; i.e., 4 degrees trailing-edge down for the canard and 6 degrees trailing-edge up for the stabilizer. The axial velocity component at 0.98 radius measured at DTNSRDC and SSPA are compared in Figure 15. The wake peak due to the strut near 0 degrees, which controls the blade cavitation, shows good agreement. Large discrepancies are shown at the blade position angle of 240 degrees. The major source of this discrepancy might be the difference in control surface angle of attack.

Cavitation inception and observation tests were performed with the optimum angle of attack of the control surfaces at the original pitch of $(P/D)_{0.7R}=0.6722$ and at the final pitch of $(P/D)_{0.7R}=0.6471$. For the original pitch, tests were performed for both model and full-scale wakes. For the repitched propeller, tests were performed only for model wake.

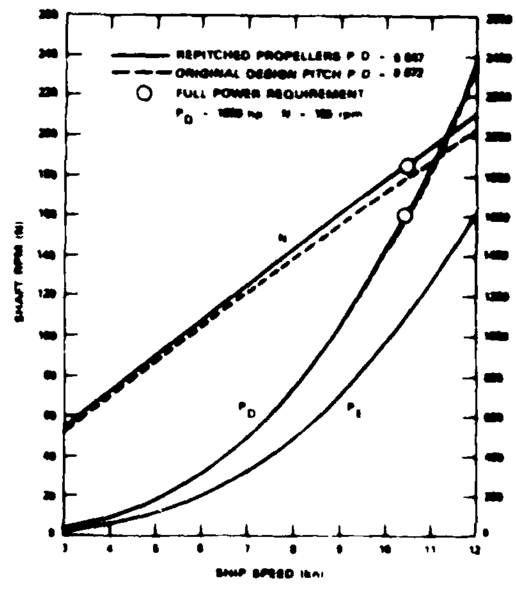

Fig. 14 Powering Performance of the Repitched Propeller

Figure 16 shows the polar diagram of the maximum radial cavitation extension at full power for model wake, and photographs reproduced from the video tapes recorded during the tests. The white spots near the leading edge between the 0.85 and 0.9 radius indicate the leading-edge sheet cavitation on the suction sides. The repitched propeller showed slightly improved cavitation performance. The cavitation erosion test results showed no erosion tendency.

8. DISCUSSION

Propeller design requires complex trade-offs to satisfy various design requirements. As demonstrated in the present design, even if the design has been carefully developed, utilizing state-of-the-art design tools, there is no guarantee that the propeller will perform as designed.

The results of the propulsion experiments with the design propellers showed that the propellers did not meet the required rpm at full power. An examination of the propeller-hull interaction coefficients showed that the Taylor wake fraction, $1-w_T$, had changed substantially between the stock and design propellers. If it had not changed, the rpm should have been close to the design rpm.

As indicated by the very low rpm from the powering tests (see Table 2) using stock propellers, the pitch of the stock propeller was substantially higher than the design propeller, as was the wake fraction. Ideally, the geometry of the stock propeller should be as close as possible to the final propeller geometry.

In general, the model wake has been used in surface-ship propeller design, assuming that scale effects are negligible. In the present design, the estimated full-scale wake was used, which was obtained by increasing the model value by 6 percent. The performance of the full-scale propeller at sea is very much dependent upon how well the full-scale wake was predicted.

9. ACKNOWLEDGEMENTS

The authors are grateful to the Propulsor Design Review Committee of Code 1544, DTNSRDC, F. Peterson, E. Caster and S. Jessup, for their discussions and critique of the design, and to Dr. O. Rutgersson of SSPA for providing them with the photos shown in Figure 16.

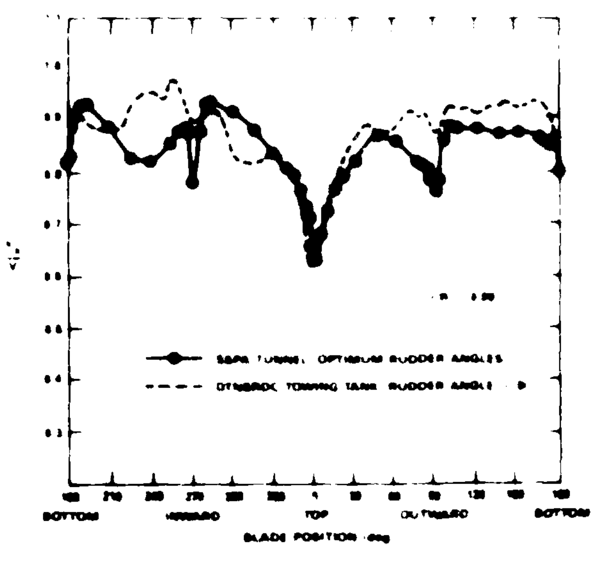

Fig. 15 Comparison of Velocity in the Propeller Plane Measured at DTNSRDC and SSPA

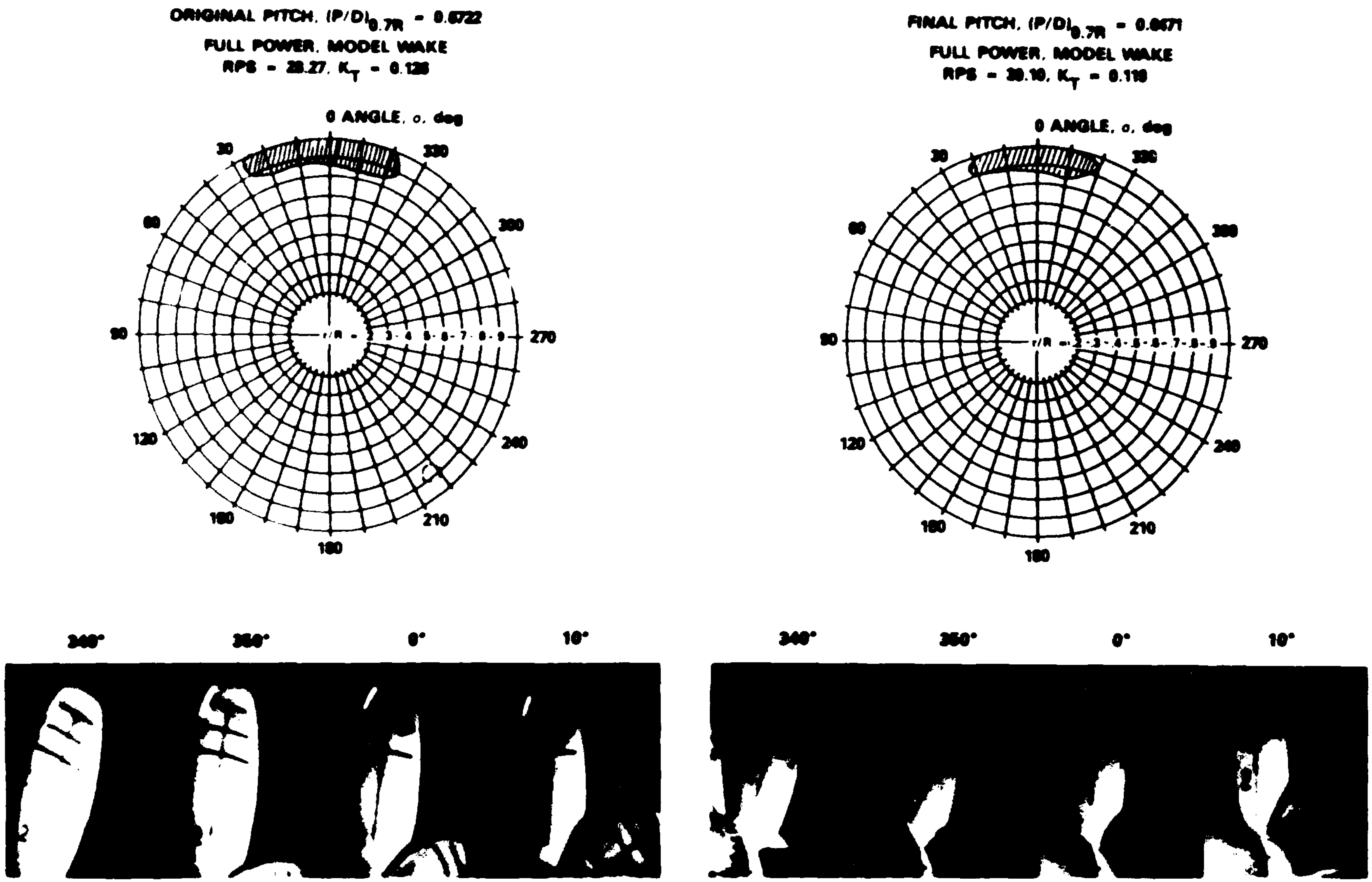

Fig 16 Maximum Radial Cavitation Extension on Original and Repitched Propellers at Full Power, Model Wake.

10. REFERENCES

1. Covich, P.M., "SWATH T-AGOS, A Producible Design," AIAA Paper No. 86-2384, Presented to the AIAA 8th Advanced Marine Systems Conference, San Diego, California (Sep. 1986).

2. Grant, J. and C. Wilson, "Design Practices for Powering Predictions," DTNSRDC Report SPD-693-01 (1976).

3. Lerbs, H.W., "Moderately Loaded Propellers with a Finite Number of Blades and and Arbitrary Distribution of Circulation," Transactions SNAME, Vol. 60 (1952).

4. Sasajima, H. and I. Tanaka, "On the Estimation of Wake of Ships," Proceedings, 11th ITTC, Tokyo (1966).

5. Huang, T.T., Wang, H.T., Santelli N. and Groves, N., "Propeller/Stern/-Boundary-Layer Interaction on Axisymmetric Bodies: Theory and Experiment," DTNSRDC Report 76-0113 (1976).

6. Brockett, T.E., "Minimum Pressure Envelopes for Modified NACA-66 Sections with NACA a=0.8 Camber and Buships Type I and Type II Sections," DTNSRDC Report 1789 (Feb. 1966).

7. "Rules for Classification and Construction of Steel Vessels," American Bureau of Shipping (1985).

8. Boswell, R.J., "Design, Cavitation Performance and Open-Water Performance of a Series of Research Skewed Propellers," DTNSRDC Report 3339 (Mar. 1971).

9. Abbot, I.H. and A.E. Von Doenhoff, Theory of Wing Sections Including a Summary of Airfoil Data, Dover Publication Inc., New York (1958).

10. Greeley, D.S. and J.E. Kerwin, "Numerical Methods for Propeller Design and Analysis in Steady Flow," Transactions SNAME, Vol. 90 (1982).

11. Kerwin J.E. and C.S. Lee, "Prediction of Steady and Unsteady Marine Propeller Performance by Numerical Lifting Surface Theory," Transactions SNAME, Vol. 86 (1978).

12. Rutgersson, O., "SWATH T-AGOS Model Tests in Cavitation Tunnel," SSPA Report No. 4397-1 (Jul. 1986).

INITIAL DISTRIBUTION

Copies	
14	NAVSEA
	1 SEA 5046 (Bauman)
	3 SEA 55W3 (Comstock, Davey, Hough)
	1 SEA 56X1 (LaFone)
	3 SEA 56X7 (Crockett, Platzer, Majumdar)
	1 SEA 5011 (Howell)
	1 SEA 5015 (Cannon)
	1 SEA 50151 (Kennell)
	1 SEA 55N3 (Lee)
	1 SEA 55N2 (Paladino)
	1 SEA 99612 (Library)
2	PMS 383 (Nunnery, Perin)
1	MSC M4E2 (Jacobson)
1	SSNO 100 (Jenkins)
1	USCG G-MSC (Reid)
1	ABS AAM/fd (Stromer)
1	NAVSHIPYD PTSMH/Lib
1	NAVSHIPYD PHILA/Lib
1	NAVSHIPYD NORVA/Lib
1	NAVSHIPYD CHASN/Lib
1	NAVSHIPYD LBEACH/Lib
1	NAVSHIPYD MARE/Lib
1	NAVSHIPYD PUGET/Lib
1	NAVSHIPYD PEARL/Lib
1	USNA/Lib
1	NAVPGSCL/Lib
1	NOSC/Lib
1	NCSC/712

Copies	
1	NSWC, White Oak/Lib
1	NUSC/Lib
12	DTIC
2	MARAD
	1 Div of Ship R&D
	1 Lib
2	MIT
	1 Baker Lib
	1 J.E. Kerwin
3	U. of Michigan (NAME Dept)
	1 Lib
	1 T. Brockett
	1 W. Vorus
1	Penn State U/ARL Lib
1	SNAME/Lib
1	Tracor, Hydronautics (S. Kobayashi)
1	Bird Johnson (J. Norton)
1	HRA Assoc. (B. Cox)
1	Atlantic Research (D. Greeley)

CENTER DISTRIBUTION

Copies	Code	Name
1	012.3	D.D. Moran
1	1235	R. Lamb
1	15	W.B. Morgan
1	1504	V.J. Monacella
1	1506	S. Hawkins
1	1508	R. Boswell

Copies	Code	Name
1	152	W.C. Lin
3	1521	W. Day G. Borda H. Liu
3	1522	M. Wilson J. Lawler K. Remmers
1	154	R. Folb
2	1542	T. Huang B. Yim
25	1544	F. Peterson K.-H. Kim (10) A. Reed (10) S. Jessup C. Schott J. Fraas N. Hubbard
1	1905.1	W. Blake
10	5211.1	Reports Control
1	522.1	TIC (C)
1	522.2	TIC (A)

END
11-87
DTIC